Chinese Chemical Letters 34 (2023) 107130

Contents lists available at ScienceDirect

Chinese Chemical Letters

journal homepage: www.elsevier.com/locate/cclet

Development prospects of metal-based two-dimensional nanomaterials in lithium-sulfur batteries

Yuxue Mo[a,b,e], Liling Liao[b], Dongyang Li[b], Rongwu Pan[d], Yanhong Deng[a], Yanliang Tan[a,*], Haiqing Zhou[b,c,*]

[a] College of Physics and Electronic Engineering, Hengyang Normal University, Hengyang 421002, China
[b] Key Laboratory of Low-Dimensional Quantum Structures and Quantum Control of Ministry of Education, Key Laboratory for Matter Microstructure and Function of Hunan Province, Department of Physics and Synergetic Innovation Center for Quantum Effects and Applications, Hunan Normal University, Changsha 410081, China
[c] Hunan Joint International Laboratory of Advanced Materials and Technology for Clean Energy, Changsha 410082, China
[d] Hunan Shengli High-tech Energy Technology Co., Ltd., Yongzhou 425000, China
[e] Hunan Provincial Key Laboratory of Intelligent Information Processing and Application, Hengyang 421002, China

ARTICLE INFO

Article history:
Received 20 November 2021
Revised 20 December 2021
Accepted 9 January 2022
Available online 15 January 2022

Keywords:
Lithium-sulfur battery
Two-dimensional materials
Cathode materials
Anode materials
Anode protection

ABSTRACT

A lithium-sulfur (Li-S) system is an important candidate for future lithium-ion system due to its low cost and high specific theoretical capacity (1675 mAh/g, 2600 Wh/kg), which is greatly hindered by the poor conductivity of sulfur, large volume change and dissolution of lithium polysulfides. Two-dimensional (2D) materials with monolayers or few-layers usually have peculiar structures and physical/chemical properties, which can resolve the critical issues in Li-S batteries. Especially, the metal-based 2D nanomaterials, including ferrum, cobalt or other metal-based composites with various anions, can provide high conductivity, large surface area and abundant reaction sites for restraining the diffusion for lithium polysulfides. In this mini-review, we will present an overview of recent developments on metal-based 2D nanomaterials with various anions as the electrode materials for Li-S batteries. Since the main bottleneck for the Li-S system is the shuttle of polysulfides, emphasis is placed on the structure and components, physical/chemical interaction and interaction mechanisms of the 2D materials. Finally, the challenges and prospects of metal-based 2D nanomaterials for Li-S batteries are discussed and proposed.

1. Introduction

For the requirements of electric vehicles and electrochemical energy storage in the present and future, rechargeable lithium-ion batteries (LIBs) have attracted considerable attention with great achievements including cathodes, electrolyte and anode protection, which are the main components and key ingredients for the energy density of LIBs [1–3]. With the expanding demands in the improved energy density and market (expected to increase by 650% in 2027), nanotechnology and advanced nanomaterials should be developed gradually to satisfy the demands [4,5]. In particular, sulfur is adopted as cathode and lithium metal as anode in the lithium-sulfur (Li-S) batteries, which has been considered as a promising next generation of electrochemical energy storage due to the low cost and high specific theoretical capacity (1675 mAh/g, 2600 Wh/kg) based on Eq. 1, corresponding to an average voltage of 2.15 V as shown in Fig. 1a.

$$S_8 + 16Li^+ + 16e^- \rightarrow 8Li_2S \quad (1)$$

Although sulfur would be the most ideal cathode material, some key obstacles should be worked out before its industrial utilization. During the discharge/charge process in Li-S batteries (Fig. 1a), there are four main reaction stages and two-phase transformation between solid and liquid [6]: Stage I: Solid S_8 is transformed into liquid Li_2S_8, which can dissolve in the electrolyte with very fast kinetics (Eq. 2). Stage II: Liquid Li_2S_8 is further converted to low-order liquid polysulfides (Li_2S_n, $4 \leq n \leq 6$), probably Li_2S_4 at the end, resulting in the increase of viscosity of the electrolyte [7], as depicted in Eq. 3. Stage III: Liquid Li_2S_4 again evolves into insoluble solid Li_2S_2 or Li_2S (Eq. 4). Stage IV: Liquid Li_2S_2 is transformed into solid Li_2S, which cannot dissolve in the electrolyte and the reaction kinetics is relatively low (Eq. 5) [8]. It should be noted that the intermediate reaction products of Li_2S_n (liquid) ($4 \leq n \leq 8$) are very vulnerable to dissolve in the ethers electrolyte, and can migrate to the lithium anode by the electric field and concentration

* Corresponding authors.
E-mail addresses: hytyl@163.com (Y. Tan), hqzhou@hunnu.edu.cn (H. Zhou).

https://doi.org/10.1016/j.cclet.2022.01.023
1001-8417/

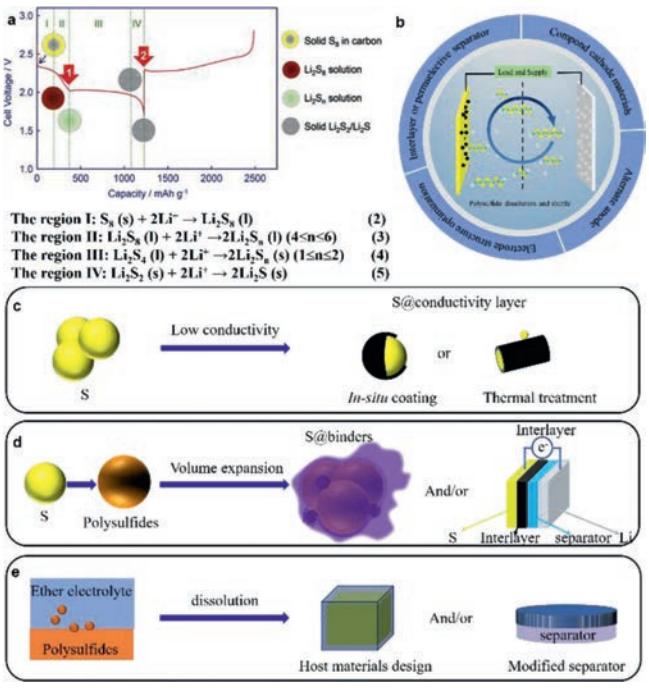

Fig. 1. (a) A typical charge/discharge curve and electrochemical evolution of Li-S batteries. Reproduced with permission [7]. Copyright 2013, Elsevier. (b) Schematic illustration of the fundamental applications of 2D materials in Li-S batteries. Some of the highlighted design strategies of host materials: (c) improving the electrical conductivity, (d) suppressing volume expansion and (e) LiPSs dissolution.

gradient [9], causing the deleterious "shuttle effect", thus leading to the degradation of Li-S batteries. Meanwhile, the increased viscosity of the electrolyte would obstruct Li^+ ion diffusion properties and the dissolved Li_2S_n can also corrode the lithium metal due to the undesirable reaction between Li_2S_n and Li anode. Additionally, due to the different density of S_8 (2.07 g/cm^3) and reaction product of Li_2S (1.66 g/cm^3), the volume expansion would reach up to 80% after lithiation [10]. In particular, the Li-S batteries suffers from the poor electronic conductivity of S_8 and reaction products of Stages I and IV (key stages), which mainly hinder the electrochemical cycling stability and usage rate of active S species, resulting in rapid capacity fading and low coulombic efficiency [10].

On the basis of aforementioned stages, controlling the dissolution of liquid Li_2S_8 and accelerating the redox reactions of Li_2S or other short-chain polysulfides would be the critical obstacles to improving the electrochemical performance of Li-S batteries. In this regard, engineering the microscopic structures and chemical compositions in S host materials is an effective and straightforward strategy to solve these issues. Therefore, considerable efforts have been devoted to searching more reliable materials to improve the electrochemical performance of Li-S batteries and narrowing the gap between fundamental research and practical applications (>6 mAh/cm^2) that the Li-S batteries have high cycling stability but low areal sulfur loading (<2 mg/cm^2, the areal capacity: <3.35 mAh/cm^2) [11–13]. As shown in Figs. 1b and c, rational design of precise components of 2D materials for S cathode materials, interlayer or permselective separator and electrode structure optimization are demonstrated to be tried and true strategies, taking consideration of low conductivity of S (5×10^{-28} S/m), volume expansion (80%) and dissolution of lithium polysulfides (LiPSs) in the ether electrolyte during cycling. Aiming at solving the aforementioned disadvantages, a series of typical methods have been developed (Figs. 1c and d). For example, highly conductive materials are commonly accepted as the ideal host materials for S species by *in-situ* coating and/or thermal treatment with S particles, so as to greatly improve the conductivity of S cathodes. Compared with the thermal treatment, it should be pointed out that the synthetic methods with *in-situ* deposition on the surface of S plays a positive role in isolating the direct contact between S species and the electrolyte, so that the majority of the S species are kept inside the S host materials, thus greatly enhancing the electrochemical stability. Meanwhile, as for the volume expansion, multifunctional binders with excellent tensile properties and/or interlayers with light weight, large specific area and rich pores are a better choice. In addition, directing to the inevitable dissolution and shuttle effects of LiPSs, emphasis is placed on the smart design of host materials for holding S species or exceptional separator with strong physical/chemical adsorption effect, strong chemical interaction and catalytic effect between the introduced materials and LiPSs (Fig. 1e). Finally, the electrode structure optimization and Li anode protection are also very important factors for the practical application of Li-S system. In this sense, the sulfur cathodes with layer-by-layer construction are a promising step further toward commercial application, where the energy density can be up to 603 Wh/kg [14], which is higher than NCR18650B (energy density: 240 Wh/kg) in Li-ion batteries [15]. Regarding the safety of Li-S batteries, Li anode protection is a challenging issue due to the heterogeneous nucleation and growth in Li plating [16].

In Li-S system, carbon-based nanomaterials, such as carbon nanofibers, carbon nanotubes, porous carbon and metal organic frameworks (MOFs) derived carbon [17,18], are excellent candidates to solve the above issues due to their good electrical conductivity, large surface area, high porosity and various structures. This is because these carbon-based nanomaterials can provide enough space for sulfur and improve the conductivity and electrochemical performance of S cathode. Even so, it is worth pointing out that carbon-based nanomaterials usually have weak chemical interaction and adsorption with LiPSs, which would result in instability of long-term cycling performance and low coulombic efficiency for Li-S batteries. Thus, additional complicated process, such as N or O doping, should be performed for these carbon-based nanomaterials, so as to induce strong chemical interaction with LiPSs, suppress the "shuttle effect" of LiPSs, and enhance the utilization of S and coulombic efficiency [19]. Unfortunately, abundant defects would be created during the functionalization process of carbon materials, which would cause chain reactions and do not benefit for the permeability of electrolyte. In this regard, in order to go a further step toward industrial applications of Li-S system, it is highly desirable to develop new technology for rational design and synthesis of new kind of electrode materials for loading S species in low cost and large scale.

Based on the above standpoints, two-dimensional metal-based nanomaterials (2D metal-based nanomaterials), which have light weight, good conductivity and large surface area, have attracted growing attention recently and become ideal platforms for Li-S batteries due to their easy functionalization and potentially scalable production [20–23]. In particular, 2D metal-based nanomaterials (Co-N-C, Mo_6S_8, *etc.*) display semiconducting and metallic behaviors [24–28], and can enable fast charge transfer and catalytic effects in the conversion reaction of LiPSs through their chemical interactions with sulfur atoms, which is in sharp contrast to the carbon-based nanomaterials. Both of them have positive effects on the final cell performance. As for the layered structures of 2D metal-based nanomaterials, it is expectedly beneficial for ion transport channels and diffusion properties [29,30]. Moreover, these materials display outstanding mechanical properties, which can withstand large stress and strain without structural collapse, and provide various supportive networks for volume expansion of S electrode materials [31]. Finally, the metal elements in 2D metal-based materials would be the reacting centers for the adsorption and decomposition with polysulfides [32], especially for single-

atom (SA) catalysts. Once they can be synthesized through controlling the preparation process and stoichiometric ratio of reaction, single-atom materials can extremely improve the utilization efficiency of metal atoms, save the resources and protect the environment [33]. Therefore, these intrinsic advantages of 2D metal-based nanomaterials make them very appealing as the host materials for S species, interlayer coated on the separator, or anode protection to address the existing challenges of Li-S batteries.

With these merits in mind, we will try to summarize the great achievements and challenges of 2D metal-based materials in the Li-S system. For the Li-S batteries, the poor conductivity and shutting effect of LiPSs are the two critical obstacles for the practical application. Although many excellent works have been reported recently on improving the diffusion and transmission properties of Li^+/electrons and inhibition of LiPSs, 2D metal-based materials can provide us some different viewpoints on solving the aforementioned challenges. For example, due to the formed "dead Li" between Li anode and polysulfides, 2D metal-based materials can improve the process of Li plating/stripping, decrease the formation of "dead Li" and finally protect the Li anode, thus improving the safety of Li-S batteries [34]. Therefore, at the first section, the key factors, intrinsic problems and their physical origins have been categorized, followed by introducing the possible strategies on solving the critical problems of Li-S batteries. At the 2^{nd}-4^{th} sections, we have summarized the recent advances on improving the electrochemical performance of Li-S batteries by employing 2D metal-based materials as the host materials for S species, interlayer/modified separator and anode protection, so as to gain further insights into the rational design and synthesis of electrode materials in Li-S system. On this basis, we can correlate the preparation methods, microscopic structures, and chemical compositions with the electrochemical performances and the possible mechanisms of polysulfide shutting prevention. At 5^{th} section, the major challenges and future research directions of two-dimensional metal-based nanomaterials in Li-S batteries have been highlighted.

2. Metal-based nanomaterials with various anions for sulfur hosts and polysulfide shutting prevention

For the Li-S batteries, the low conductivity of S species and the reaction products of solid Li_2S_n ($1 \leq n \leq 2$) are the basic obstacles, which can cause an aggravation of the electrochemical process and decreased capacity [31]. Based on this point, considerable efforts have been devoted to utilizing carbon-based materials for improving the conductivity of S electrode [35]. Due to the dissolution of Li_2S_n ($3 \leq n \leq 8$) and weak adsorption effect of carbon-based materials, the increased viscosity of the electrolyte would decrease the Li^+ transmission, and increase the internal resistance of the electrode. In this regard, it is highly significant to design the component and architecture of S host materials to improve the electrode conductivity and polysulfide imprisonment.

2.1. Ferrum-based 2D nanomaterials

The utilization of various carbon-based materials, *i.e.*, carbon nanotubes, carbon nanofibers and 3D hyperbranched hollow carbon can decrease the interfacial contact resistance and the polarization of the battery. Due to the weak interactions between sulfur and the carbon-based materials, LiPSs could not be efficiently anchored on internal electrodes, and very few reaction sites can be provided for the adsorption of LiPSs even though these carbon-based materials have been functionalized with N [36], O [37–39] and B [40–42]. Especially, the shuttle effect is still a big challenge. Accordingly, ferrum-based 2D nanomaterials, such as iron hydroxides, sulfides, nitrides and oxides, have large specific surface areas, layered structure and abundant electrochemical reaction sites, which can improve the conductivity of the sulfur cathode and provide plentiful reaction sites for the conversion of LiPSs [35]. Particularly, ferrum-based 2D nanomaterials with various anions ($FePS_3$, Fe/Fe_3C, $Fe_{1-x}S$@NC, *etc.*) could have intensive chemical adsorption for polar polysulfide species and trap the polysulfides on the electrode [43–45], thus reducing the dissolution in the electrolyte and enhancing the electrochemical reaction kinetics.

The utilization of transition metal oxides can be beneficial for the adsorption of LiPSs. For example, Zhang *et al.* verified the Fe-vacancies could provide adsorption sites and promote the chemical interactions for LiPSs, which can serve as an efficient catalyst to accelerate the conversion reactions [46]. On the basis of these points, Li *et al.* designed an FeOOH nanorods/EG composite by a hydrothermal method to suppress the shuttle effect and enhance redox kinetics of Li-S battery (Figs. 2a-c), which exhibits a small polarization ($\triangle E = 0.19$ V) and a high reversible capacity of 733 mAh/g after 500 cycles at 2 C [47]. Xie *et al.* synthesized thin PDA-coated FeOOH (PDA@FeOOH) nanospindles and then performed heat treatment and HCl etching for the PDA@FeOOH, so as to create extra void spaces, which can avoid the volume expansion during lithiation [37].

Due to the low cost, easy production in large scale and good electrochemical performance discussed above, ferrum-based 2D nanomaterials have attracted extensive attention. Li *et al.* synthesized Fe_3C-MC composite with a loose fiber chain structures by a pyrolysis method (Figs. 2d and e), which displayed excellent performance at high sulfur loading (up to 9 mg/cm^2) (Fig. 2f). This could provide a promising and novel strategy for commercial applications of Li-S batteries [48]. As shown in Figs. 2g and h, Qiu *et al.* designed and synthesized Fe-NC material, and the results of EXAFS demonstrate that Fe atoms are coordinated with two N atoms, where Fe-N_2 sites were formed (Figs. 2i-l) [49]. Due to bifunctional Fe-N_2 sites, LiPSs were strongly anchored on the electrode, and the reversible conversion from S_8 to Li_2S was accelerated, which can be attributed to the catalytic effect of the metal center and the reduction of the reaction energy barrier for Li_2S decomposition. This interesting point could activate the investigation of transition metal-nitrogen carbon (M-NC) catalysts for long-term Li-S batteries, such as Fe-N, Fe-Ni-P@NC, FeHCF-A and Fe-Ni@NC [50–53]. For instance, Zhou *et al.* revealed the ability of capture and conversion between LiPSs and single-metal atoms by theoretical calculations [54], which provides a useful guide for growing single-metal-atom materials (*i.e.* FeSA-CN, Fe-PNC) [55,56] for improving the stability of Li-S batteries.

2.2. Cobalt-based 2D nanomaterials

As mentioned above, Fe-based 2D nanomaterials have shown electrocatalytic ability to improve the conversion kinetics for polysulfides and provide reaction sites for adsorbing Li_2S_n ($1 \leq n \leq 8$), where the metal center plays an important role in these processes. Thus far, there is a growing interest in polar and catalytic materials made of other transition metal-based compounds, which could potentially address the polysulfide shutting effect and long-term stability by promoting chemical interactions between polysulfides and metal centers [57]. Recently, cobalt-based 2D nanomaterials (*e.g.*, Co_3O_4/Co-NC600 [57], Co_3S_4 [58], Co_3S_4 [59]) have been demonstrated to have electrocatalytic ability to increase the reaction kinetics between the solid and liquid polysulfides [60]. On this basis, Wang *et al.* reveal that CoOOH nanocubes with a regular hexagon structure (Figs. 3a and b), which exhibit outstanding electrocatalytic activity and electronic conductivity, and have a strong adsorption for soluble intermediate [61]. The good performance is ascribed to S-Co bond formation and abundant metal centers as the active sites for electrochemical reactions, which can help the electrode materials to anchor polysulfide and suppress polysulfide

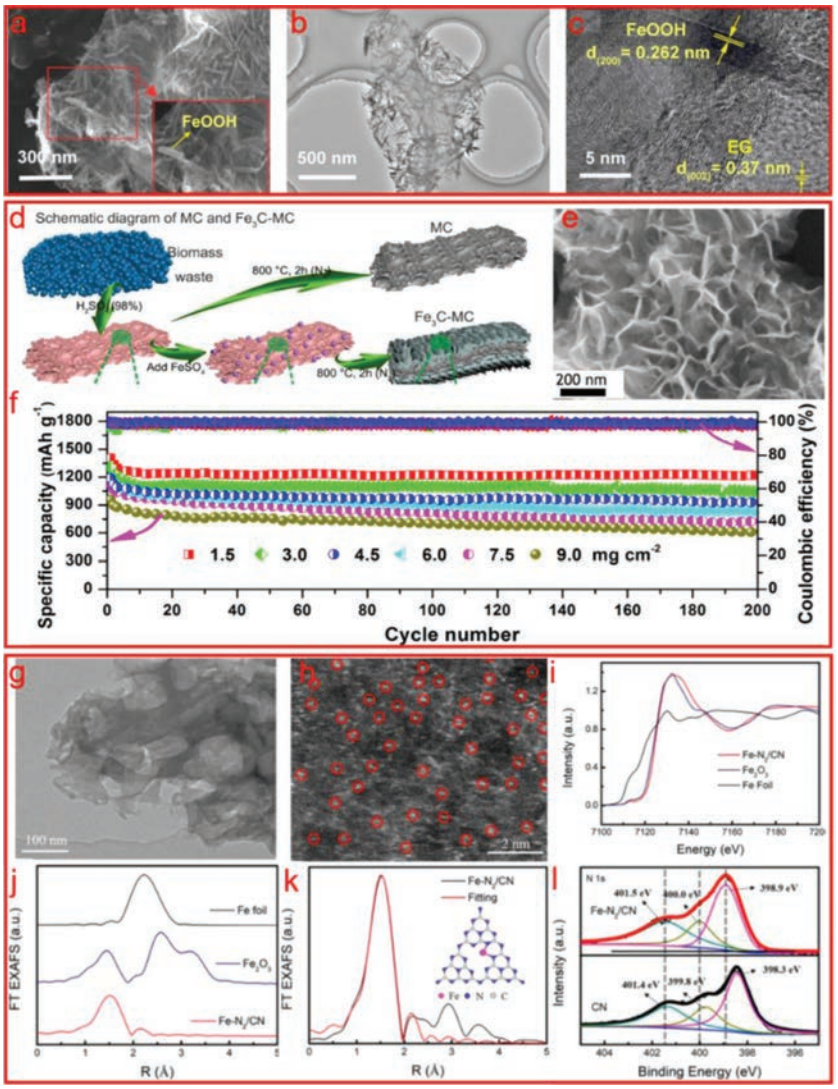

Fig. 2. (a) SEM and (b, c) TEM images of FeOOH/EG-S composite. Reproduced with permission [47]. Copyright 2020, Royal Society of Chemistry. (d) Scheme of the preparation method. (e) SEM and (f) cycling performance of Fe_3C-MC/S at 0.5 C. Reproduced with permission [48]. Copyright 2018, Elsevier. (g) TEM and (h) HAADF-STEM images of Fe-N_2/CN. (i) Fe K-edge XANES spectra. (j) Fourier transforms of Fe K-edge EXAFS spectra. (k) r-space EXAFS fitting curve (inset: the top view of the Fe-N_2 coordinated structure; gray (C), magenta (N), blue balls (Fe)) and (l) XPS spectra of N 1s of CN and Fe-N_2/CN. Reproduced with permission [49]. Copyright 2020, American Chemical Society.

diffusion from the cathode [61–64]. Mo *et al.* reported a high-performance S@$Co(OH)_2$ composite material with 80% S content, where the $Co(OH)_2$ nanosheets were *in-situ* deposited on S surface by one-step wet chemistry [65]. The outer $Co(OH)_2$ shell acts as a physical barrier preventing polysulfides from leaking into the electrolyte, and also contributes to the catalytic decomposition of polysulfides during the cycling process. In these works, the Co atoms are the react centers and have strong chemisorption for polysulfides by forming S-Co bonds.

In order to further improve the conductivity of S species, metallic Co-based compounds are a better choice. Sun *et al.* synthesized metallic cobalt nitride (Co_4N; particles on metal organic framework-derived nanocages denoted as h-Co_4N@NC (Fig. 3c) where a hollow nanocage structure was used as the S host [66]. In this way, the Co_4N is found to exhibit better catalytic activity compared to metallic Co catalyst, which can catalyze LiPSs conversion and inhibit the shuttle effect by enhanced trapping and adsorption of LiPSs (Fig. 3d), endowing the h-Co_4N@NC/S electrodes with small electrochemical polarization, excellent rate capabilities and long-term cycling performance (Figs. 3e and f) [66]. Yang *et al.* demonstrated that numerous Co-N_x coordination sites synergistically catalyze the formation of LiPSs converted from active sulfur species with high efficiency, thus reducing the voltage polarization. Therefore, based on these strategies, polysulfide shuttling can be mitigated and the coulombic efficiency is improved by higher Co or N content [67].

In addition to the electrical conductivity, more and more people have paid much attention to the utilization efficiency of metal atoms. Zhao *et al.* [27] further adopted an advanced strategy of double-end binding (DEB) sites to effectively immobilize the LiPSs by combining polar ZnS nanoparticles and Co-N-C single-atom centers (Fig. 3g), which can bind with the negatively charged end S_n^{2-} and positively charged end Li^+ (Figs. 3h and i). They further reveal that the electrochemical performance of Li-S batteries is superior to $LiNi_xCo_yMn_{1-x-y}O_2$ cathodes, and a pouch cell (a single-piece cathode, 100 mg sulfur loading) still exhibits a high specific capacity of 800 mAh/g (Fig. 3j). These findings demonstrate that the DEB sites can effectively immobilize the dissolved LiPSs and further boost the electrochemical S redox kinetics due to its excellent immobilization and catalytic effect [27]. It is obvious that the

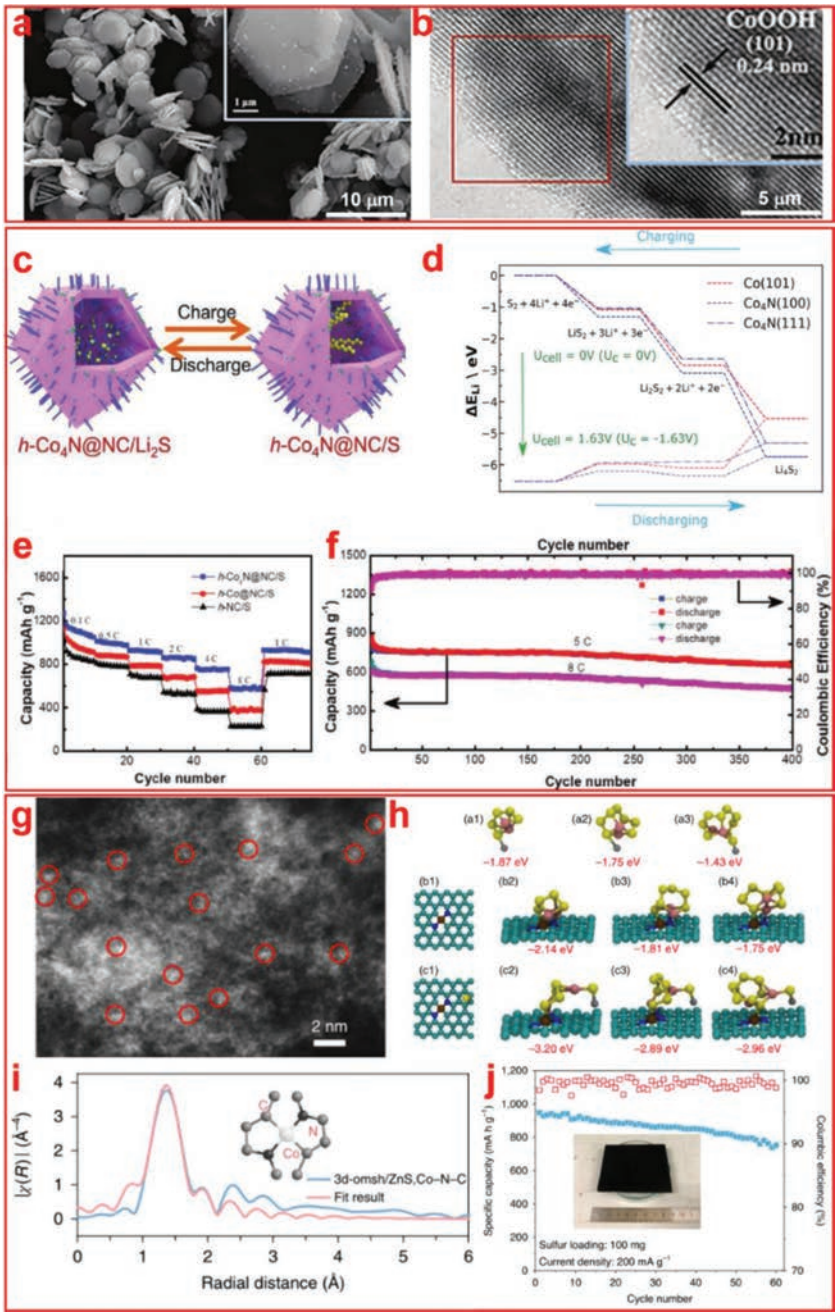

Fig. 3. (a) SEM and (b) HRTEM images of a CoOOH sheet. Reproduced with permission [61]. Copyright 2019, Wiley-VCH Verlag GmbH & Co. KGaA, Weinheim. (c) The schematic diagram of the h-Co_4N@NC/S synthesis, (d) free energy route for lithiation on the surfaces at x = 2, (e) rate performance and (f) cycling performance of the h-Co_4N@NC/S. Reproduced with permission [66]. Copyright 2020, Wiley-VCH Verlag GmbH & Co. KGaA, Weinheim. (g) TEM of the Co-N-C. (h) optimized configurations of LiPSs absorption on (a1–a3) ZnS, (b1-b4) Co-N-C and ZnS, (c1-c4) Co-N-C surface (yellow: S, pink: Li, silver: Zn, brown: Co, blue: N, cyan: C). (i) Co K-edge EXAFS of the 3d-omsh/ZnS, Co-N-C and (j) cycling performance of 100-mg-sulfur pouch cell (3d-omsh/ZnS, Co-N-C/S cathode). Inset: cathode size: 6 cm × 8 cm cathode. Reproduced with permission [27]. Copyright 2020, UChicago Argonne, LLC, Operator of Argonne National Laboratory under exclusive license to Springer Nature Limited.

increased content of Co, N or other polar elements in the S cathode can provide more reaction or adsorption sites for suppressing the dissolution/diffusion and also accelerating the electrochemical conversion process of of LiPSs [68]. Among these functional materials, single-metal atoms embedded in 2D materials usually have special properties based on the relationships between the structure and catalytic activity, which could work out the issues of Li-S batteries [69,70].

Actually, excluding the conductivity, reaction centers and atom utilization efficiency, there are some other important factors playing positive roles in the final electrochemical performance of Li-S batteries, such as the exposure of reaction centers and defects. Du *et al.* identified that the exposure of catalysts (Co-N/G) to residual reactants is a key factor to affect the kinetic process of the reaction [71]. Wang *et al.* further performed theoretical simulation and confirmed that the introduced N atom can increase the charge number of Co central atoms and create new defect levels, which can shift the Co 3d band closer to the Fermi level and eventually facilitate the conversion of LiPSs and Li_2S oxidation reaction [72].

2.3. Other metal-based 2D nanomaterials

Except for the Fe and Co-based 2D nanomaterials, there are a large number of host materials for supporting S species, such

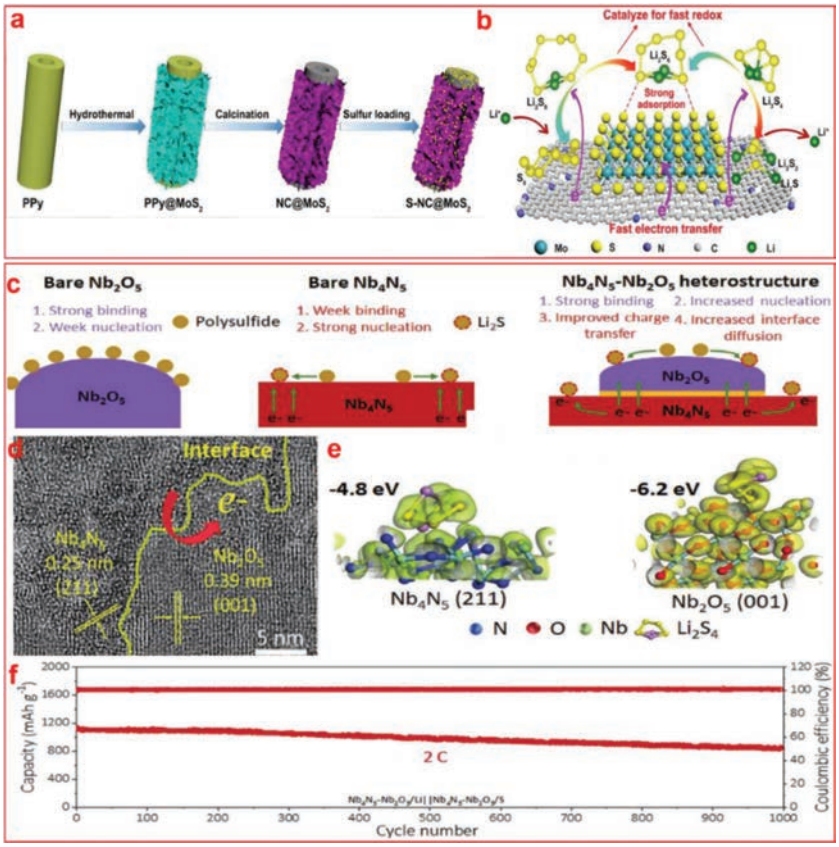

Fig. 4. (a) Scheme of the synthesis process and (b) the polysulfide adsorption and conversion processes on the surface of NC@MoS_2. Reproduced with permission [77]. Copyright 2019, Royal Society of Chemistry. (c) Schematic configuration of catalytic mechanism and the heterostructure of Nb_4N_5-Nb_2O_5 based on Li-S full cells, (d) TEM, (e) binding energies of Li_2S_4 on Nb_4N_5 (211) and Nb_2O_5 (001) surfaces and (f) cycling performance of Nb_4N_5-Nb_2O_5/Li||Nb_4N_5-Nb_2O_5/S battery at 2 C. Reproduced with permission [80]. Copyright 2021, Wiley-VCH GmbH.

as V_2C [73], SnO_2 [74], Ti_3C_2 [75], MoB [76], which are promising approaches to solve the polysulfide shuttling effect. Yang *et al.* synthesized an architecture of ultrathin MoS_2 nanosheets (around 11 S-Mo-S layers) supported on N-doped carbon (Figs. 4a and b). These ultrathin MoS_2 nanosheets can provide many polar sites, strong Mo-S interaction and decreased charge-transfer resistance for LiPSs [77]. Liu *et al.* analyzed the density of states (DOS) and the interfacial redox reaction kinetics of M-S_x (M: W, Co and Ni atoms), certifying that the d band of metal atoms is changed when M atoms interact with Li_2S_4 [78]. The improved redox reaction kinetics is mainly ascribed to the charge compensation from the d band of M atom to the adsorbed LiPSs, which could benefit a lot for the electron transfer and promote the LiPSs interfacial redox and conversion kinetics [78]. Zhou *et al.* confirmed the charge-transfer resistance was related to the oxidation state of Ti_3C_2 and Ti_3C_2 electrodes caused by surface groups [79]. Shi *et al.* synthesized 2D heterogeneous Nb_4N_5-Nb_2O_5 composite, in which polar Nb_4N_5 has high electrical conductivity and bare Nb_2O_5 has desirable chemical adsorption of LiPSs [80]. This unique strategy can greatly decrease the unusable electrochemical phases ("dead sulfur"). As shown in Figs. 4c-f, the Nb_4N_5-Nb_2O_5 heterostructure for both S cathode and Li anode for full-battery displays very good rate performance, high discharged capacity and excellent capacity retention ratio of the capacity, suggesting the fast reaction kinetics of the full batteries. Furthermore, the Nb_2O_5–Nb_4N_5/Li || Nb_2O_5–Nb_4N_5/S full battery can deliver a stable cycling capacity with a practicable areal capacity of 5.0 mAh/cm^2 (sulfur loading: 6.9 mg/cm^2) with high-temperature affordability and long-term cycling stability, exceeding the common Li-ion batteries (4 mAh/cm^2).

Generally speaking, once the S host materials are composed of transition metal (Fe, Co, W, Nb, *etc.*)-based compounds, the metal atoms serve as the reaction sites or centers for LiPSs, resulting in great improvement of the electrochemical performance of Li-S batteries relative to pure carbon-based materials (Table 1). Prominently, the microscopic structures of the 2D metal-based nanomaterials as the S hosts play an important role in the electrochemical properties. Among different structures, the flower-like or porous structures could be more effective to decrease the reaction energy barriers and achieve inhibition of LiPSs, thus improving the cycling performance of Li-S batteries [81,82]. On the other hand, heterostructure engineering is a good choice to improve the electrical conductivity and provide enough reaction centers for LiPSs, both of which can contribute greatly to the final electrochemical performance of Li-S batteries.

3. Metal-based nanomaterials for modified separator/interlayers and polysulfide shutting prevention

Although developing host materials for S cathode from 2D metal-based nanomaterials is an effective and straightforward strategy to suppress polysulfide shutting effect, it is worth noting that the liquid polysulfides (Li_2S_n, $4 \leq n \leq 8$) would inevitably escape from the S host materials and cathode, and diffuse through the separator to Li anode, which is arisen from the high solubility of Li_2S_n ($6 \leq n \leq 8$). Compared with the "inside" strategies for the cathode, engineering the interlayer/modified separator for Li-S batteries is considered to be an alternative "outside" strategies to block the leakage of liquid polysulfides, and obstruct its diffusion path. As discussed above, an excellent S host materials should

Table 1
The cycling performance of different 2D metal-based nanomaterials with various microscopic structures and chemical compositions.

Host materials	Structure	S content (wt%)	Sulfur loading (mg/cm^2)	E/S ratio (μL/mg)	Cycle No.	Specific capacity (mAh/g)	Capacity decay (%)	Ref.
$Fe_{3-x}C$@C	Spherical and hollow	74	Unknown	Unknown	1000 at 1 C	520	0.04	[46]
FeOOH	Nano-rod	80	2.74	5	500 at 2 C	733		[47]
Fe_3C-MC	Nanosheets	80	9.0	6	100 at 0.5 C	699		[48]
Fe-N_2/CN	Porous	70	5.6	Unknown	100 at 0.2 C	964		[46]
FeSA-CN/S	Nanocage	70	1.4	14	200 at 0.5 C	796	0.068	[55]
Fe−Ni@NC	Hexagonal close-packed	86	4.10	8	800 at 1 C	600	0.05	[56]
Co_3S_4	Nanocubes	74	7.4	5−15	1000 at 5 C	850	0.0137	[58]
CoOOH	Nanocubes	93	1.0–1.3	8-10	100 at 0.2 C	788.4	0.29	[61]
h-Co_4N@NC	Nanocubes	75.5	4.5	Unknown	400 at 2 C	516	0.06	[66]
Co−N/G	Nanocages	90	2.0	10	500 at 1 C	681	0.053	[71]
MoB	Porous	72	3.2	15	1000 at 1 C	600	0.03	[76]
Nb_4N_5–Nb_2O_5	Heterostructure nanosheet	80	1.0	10	120 at 0.2 C	1021	0.07	[80]
WS_2@NC	Flower-like	73.3	2.5	Unknown	500 at 0.1 C	1107	0.026	[82]

possess good electrical conductivity, abundant reaction sites and atomic-level dispersion [83]. Therefore, it is highly desirable to design and synthesize conductive materials as the modified separator/interlayer, so as to block the leakage of the liquid polysulfides. In the following, we will pay much attention to this kind of "outside" strategies.

3.1. Ferrum-based 2D nanomaterials for modified separator/interlayers

Apart from the S host, various 2D metal-based nanomaterials are used as interlayers or to modify the separator, aiming at suppressing the volume expansion and stress accumulation during the cycling process in Li-S batteries. Qiao *et al*. reported that the FeCFeOC composites have strong chemisorption and catalytic ability with a quick conversion reaction for the LiPSs, which would firstly adsorb and anchor on the surface of the FeCFeOC (Fig. 5a) [84]. For the reason, they proposed that magnetic FeS_x species are formed due to the reaction between Fe_xO_y and LiPSs, further inhibiting the diffusion of LiPSs (Fig. 5b). Ma *et al.* embedded single-atom (SA)-Fe and polar Fe_2N in nitrogen-doped graphene (SA-Fe/Fe_2N@NG), finding that the content ratio of SA-Fe in the composites has a great influence on the selective adsorption-catalysis behavior of LiPSs (Figs. 5c and d) [85]. For the SA-Fe/Fe_2N@NG modified separator (Area loading: 0.1 mg/cm^2), a capacity retention of 80.42% was obtained after 200 cycles at 0.2 C, much higher than those of the PP (61.92%) and SA-Fe@NG-modified separators (70.46%) [85]. A free-standing graphited carbon interlayers modified with Fe/Fe_3C was fabricated using *in-situ* method by Zhang *et al*., which is demonstrated to exhibit excellent redox kinetics and good electrical conductivity. This special process not only makes Fe/Fe_3C contact well with soluble intermediate polysulfides, but also accelerates electrochemical kinetics of the sulfur species [86]. Additionally, in order to investigate the effects of multiple components, Pan *et al*. developed ultrathin Fe_3C-N-rGO@polypropylene separator with real mass loading 0.16-0.2 mg/cm^2 (the specific surface area of Fe_3C-N-rGO: 250. 68 m^2/g, the thickness: 10 μm) [87]. Fe_3C-N-rGO can entrap LiPSs, decrease the loss of active material (capacity retention of 93.2% after 100 cycles at 0.5 C) and enhance the high rate performance (580. 5 mAh/g at 4 C).

Considering that a large surface area of the interlayers/separators is very significant for the electrochemical properties of Li-S batteries, incorporating Fe-based nanomaterials with porous N-doped carbon network (NPCN) would be a promising route to facilitate the redox reaction of polysulfides, where the N atom presents a polar surface for polysulfide adsorption (Figs. 5e and f) [88]. Zhao *et al*. proposed a novel dual-functional strategy to fabricate Fe_3O_4/HPC cathode and FeP/HPC modified separator by a process of freeze-drying/pyrolysis and phosphating [89], respectively. Due to the synergistic effects of dual-catalysts, a high coulombic efficiency (CE) and excellent cycling stability (the reversible capacity was 562.4 mAh/g at 1 C after 1000 cycles) were achieved. Even with a high areal sulfur loading of 5.73 mg/cm^2 (discharge rate of 0.01 C), the cells can still display a high CE of 97.3% and low shuttle factor of 0.08 [89]. Meanwhile, a trifunctional modified separator with FeTaPc@rGO can also provide polysulfide permselectivity and enable catalyzed cathode sulfur redox [90]. Wang *et al.* designed a modified separator consisting of conductive graphitic carbon nitride/ketjen black (g-C_3N_4/KB) layer and FeOOH layer (denoted as G-SFO) for the first time (Fig. 5g) [91], which is confirmed to have excellent physical properties with a thickness of 12.1 μm, greatly enhancing the cycling performance with a low fading rate of 0.055% per cycle after 900 cycles at 1 C. Consequently, Fe-based 2D nanomaterials have a great influence on the cycling performance of Li-S batteries and Fe element has the features of widely source and lower price, which can be easily accessible for large-scale production.

3.2. Cobalt-based 2D nanomaterials for modified separator/interlayers

Cobalt-based 2D nanomaterials with various anions are also under intensive investigation for modifying the separator. Typically, N, S, O, B and functional groups can have a coordination effect on enhancing the chemical interactions between Co atoms and the soluble polysulfide species, making the "dead" S species reused for Li-S batteries [68]. Guan *et al*. adopted a low-cost chemical reaction to synthesize the Co_2B@MXene heterostructure as the interlayer material for Li-S cells, revealing that the transfer of electrons from Co_2B to MXene is greatly improved, further boosting the redox kinetics of LiPSs and enhancing the long-term cycling performance (Figs. 6a and b) [92]. Hu *et al*. introduced reduced graphene oxide (rGO) to wrap nanostructured $CoIn_2S_4$ particles (CIS), which was served as the catalyst to boost the polysulfide conversion kinetics [93]. This process can greatly improve the electrical contact between the catalyst and electronic conducting network (areal loading: 0.72 mg/cm^2 and the thickness: 44.1 mm), thus reducing the energy barrier for the transformation of Li_2S_4 to Li_2S, and accelerating the conversion kinetics (Figs. 6c and d). Lin *et al*. constructed nickel cobaltite/carbon nanofiber ($NiCo_2O_4$/CNF) composites as a chemical trapper and conversion accelerator for LiPSs (Fig. 6e) [94], which is a good enhancer for Li^+/e^- transport and conversion reactions of solid (sulfur)-liquid (polysulfides) (Figs. 6f-h). The $NiCo_2O_4$/CNF-based batteries exhibit an excellent capacity retention of 95% after 200 cycles (at 0.1 C, sulfur loading of 6.3 mg/cm^2, Fig. 6i). Wang *et al*. designed CoS_2 nanoparticles (CoS_2/NSCNHF) modified separator to surmount the obstacles of Li-S system, which

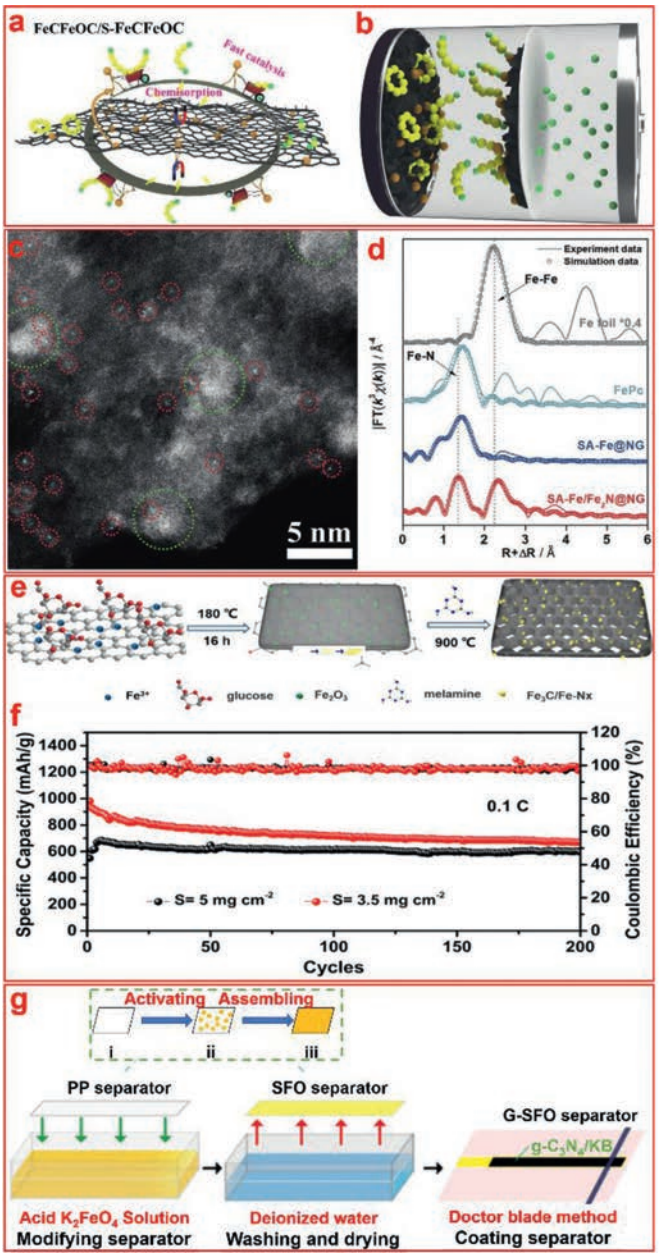

Fig. 5. (a) Schematic illustrations of the conversion process of sulfur on the surfaces of FeCFeOC and (b) the scheme of discharge/charge processes for FeCFeOC/S–FeCFeOC batteries. Reproduced with permission [84]. Copyright 2021, Wiley-VCH GmbH. (c) Single-atom Fe supported on NG characterized by TEM and (d) FT-EXAFS. Reproduced with permission [85]. Copyright 2021, Wiley-VCH GmbH. (e) Scheme of the preparation process, (f) cycling performance of the Fe_3C/Fe-N_x@NPCN-PP cells (sulfur loadings: 3.5 and 5 mg/cm^2) at 0.1 C. Reproduced with permission [88]. Copyright 2019, American Chemical Society. (g) Scheme of the fabrication of the SFO separator and the G-SFO separator. Reproduced with permission [91]. Copyright 2020, American Chemical Society.

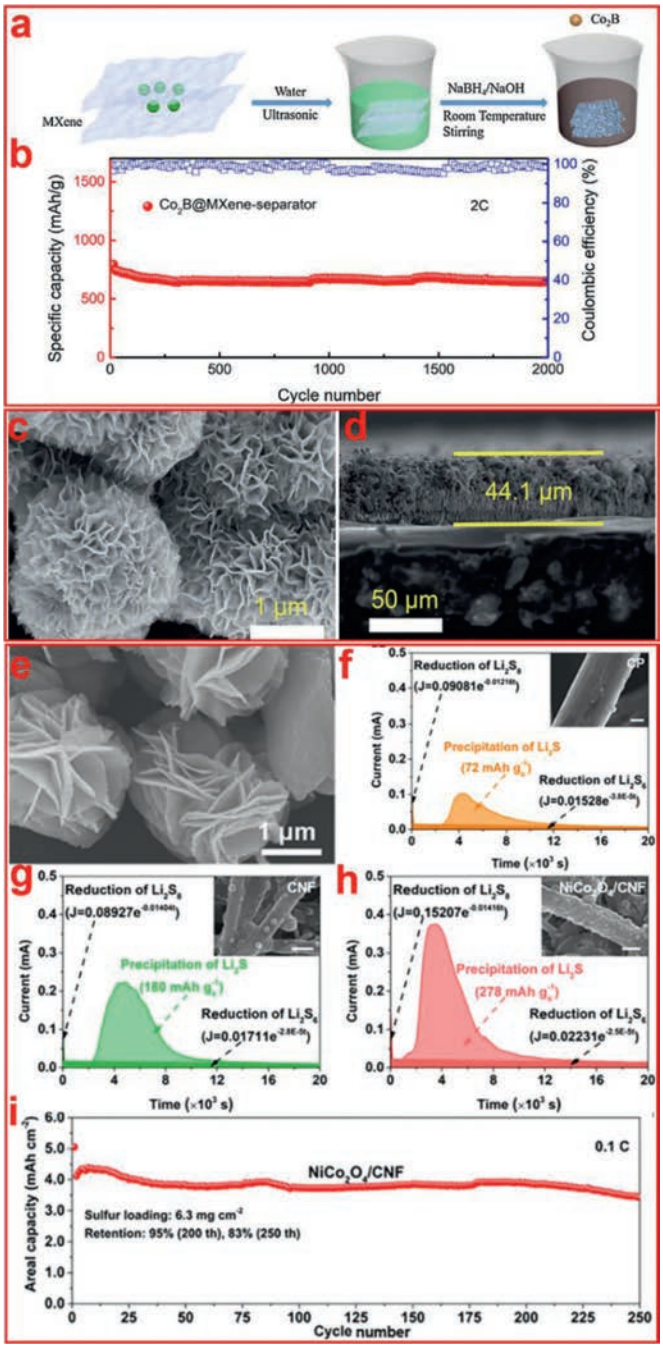

Fig. 6. (a) The illustration of Co_2B@MXene synthesis and (b) long-term cycling performance of Co_2B@MXene at 2 C. Reproduced with permission [92]. Copyright 2021, Elsevier. (c) SEM of CIS and (d) cross-section of the CIS600/RGO layer. Reproduced with permission [93]. Copyright 2021, Royal Society of Chemistry. (e) SEM of $NiCo_2O_4$, (f-h) potentionstatic discharge curves of the Li_2S_8 solution at 2.08 V on CP, CNF and $NiCo_2O_4$/CNF surfaces and (i) cycling performance at 0.1 C. Reproduced with permission [94]. Copyright 2021, American Chemical Society.

can obviously enhance electrolyte affinity and flame retardancy, and deliver an enhanced battery safety [95]. In order to improve the efficiency of metal atom utilization, implanting atomic cobalt in supramolecule-derived carbon is possibly a feasible strategy to improve the interactions between cobalt atoms and polysulfides and the electrocatalytic activity toward sulfur redox reactions [96]. Even though the electrochemical properties of Co-based 2D nanomaterials are somewhat better than that of Fe-based 2D nanomaterials, we should note that the development of Co-based 2D nanomaterials suffers from high cost, toxicity of human environment and less resources.

3.3. Other metal-based 2D nanomaterials for modified separator/interlayers

Apart from Fe and Co-based 2D nanomaterials, other metal-based 2D nanomaterial or multi-component composites were also investigated [97,98]. As shown in Fig. 7a, an ultrathin atom-thick

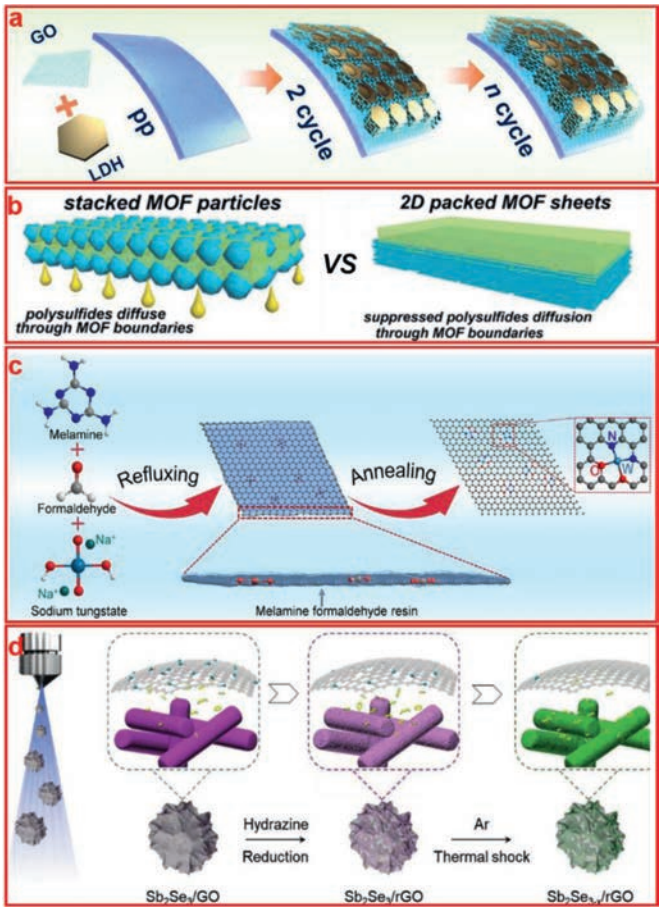

Fig. 7. (a) Schematic illustration for the process of MgAl LDH/GO ultrathin films on PP separator. Reproduced with permission [99]. Copyright 2020, Royal Society of Chemistry. (b) Schematic diagram of grainy MOFs and 2D MOF sheets in restraining the diffusion of LiPSs. Reproduced with permission [100]. Copyright 2021, Royal Society of Chemistry. (c) Scheme of the synthesis of W/NG. Reproduced with permission [108]. Copyright 2021, Wiley-VCH GmbH. (d) Scheme of the preparation of the Sb_2Se_{3-x}/rGO. Reproduced with permission [109]. Copyright 2019, Wiley-VCH Verlag GmbH & Co. KGaA, Weinheim.

film consisting of exfoliated MgAl-LDH nanosheets and GO nanosheets was constructed though a layer-by-layer assembly method, which has a great effect on stabilizing the integral structure of S cathode and inhibiting the diffusion of LiPSs [99]. Chang *et al.* synthesized closely packed laminar-like 2D CuBDC sheets to suppress the "shuttle effects" of LiPSs and improve the transport kinetics of Li^+ ions by means of a special triple-layer bottom-up method (Fig. 7b) [100]. Xu *et al.* prepared a rGO/MoO_2 modified separator with a mass loading of 0.17 mg/cm^2, where the conversion efficiency of LiPSs can be improved by the two functionalized components [101]. In particular, several pioneer works demonstrated that electrocatalysis of metal-based electrocatalysts, such as dual-function Cr_3C_2 [102], CeO_2 decorated graphene (CeO_2@G) [103], TiS_2 [104], and VSe_2 [105] could effectively promote the electrochemical performances and ensure the long-cycling stability of Li-S batteries.

MXene is a new emerging material for modifying the separator of Li-S batteries due to its metallic feature, which can greatly improve the conductivity of S species, thus boosting the electrochemical properties. Li *et al.* firstly employed ionic-covalent organic nanosheets on MXene to modify the separator, so as to mediate the redox kinetics and shuttle effect of LiPSs through the electrostatic attraction and catalytic effect [106]. The Li-S cells are optimized to exhibit a high initial capacity of 1280 mAh/g at 0.1 C and a low average capacity decay rate of 0.006% per cycle after 2000 cycles at 2 C. Even loading high sulfur content (7.6 mg/cm^2), a high reversible capacity and areal capacity were obtained. Individual and multilayered 2D $Ti_3C_2T_x$ MXene modified separators were utilized to suppress the diffusion of polysulfides, which have positive effects on the final electrochemical performance even when the S mass loading is very small (0.016 mg/cm^2) [107].

As mentioned above, single-atom catalysts (SACs) for LiPSs have higher atom utilization (100%) and can provide more electrocatalytic centers relative to particles or thin films. Wang *et al.* proposed a novel kind of tungsten (W) SAC as the adsorbent and catalyst of LiPSs (Fig. 7c), which was deposited on nitrogen-doped graphene, leading to much lower Gibbs free energy of the W/NG (1.549 eV) than NG (1.957 eV) for Li_2S_4/Li_2S conversion [108]. Tian *et al.* introduced a facile and scalable spray-drying method to grow atomic defect-rich Sb_2Se_{3-x} on reduced graphene oxides with multifunctional LiPSs barrier and abundant electron/ion transfer channels [109], which can greatly inhibit LiPSs shuttling and boost battery performance (Fig. 7d).

4. Metal-based 2D nanomaterials for anode protection

The shuttle effect is a critical issue for Li-S batteries mainly because of high solubility of reaction intermediates (Li_2S_n, $4 \leq n \leq 8$) in ether electrolyte. Due to the inevitable shuttle of LiPSs in working cells between the S cathode and Li anode, the short-chain LiPSs (Li_2S_n, $2 \leq n \leq 4$) would deposit and react with Li anode, which can result in the corrosion of Li anode and heterogeneous Li plating/stripping. This would further accelerate the formation of "dead Li" and capacity fading of Li-S batteries (Fig. 8a) [110]. In order to suppress Li dendrite, there are several approaches to realize this purpose. On one hand, some people tried to alloy Li with other metals. Luo *et al.* [111] adopted an electroless plating method to *in-situ* generate Li-Sn alloy, which can realize uniform Li nucleation/growth and reduce the nucleation overpotential (Fig. 8b). On the other hand, depositing some conductive materials on the Li anode is another effective approach to control the nucleation and growth of Li dendrites. Liu *et al.* [112] reported the mineral xonotlite ($Ca_6Si_6O_{17}(OH)_2$) nanowires (XNs) were beneficial for the homogenizing growth of Li^+ and alleviating the dendrite-caused safety of Li anode, due to its strong affinity of electrolyte and high flame-retardant property (Fig. 8c). Additionally, modifying the separator with conductive materials at the anode side is also an attractive method. With the purpose of reducing the energy barrier for Li-ion diffusion, inserting a ferroelectric decoration layer of $BiFeO_3$(BFO) at the anode side to construct an internal polarization field is a suitable strategy to control the nucleation and growth of lithium deposition [113]. However, all the above approaches require complicated fabrication processes. With this point in mind, Cui *et al.* proposed to coat a natural agar polymer (marked: A-Li) at the interface of Li anode [114], which is also competent for suppressing the volume expansion and the growth of dendritic lithium (Fig. 8d). Unfortunately, these "hostless" strategies mainly devote to modify the electrochemical properties of the Li anode interface, and the volume changes of Li anode at high current densities are still inevitable. To avoid the volume change, the "host" strategy is a promising choice, where the lithium metal is melted into the host materials, such as 3D metal porous materials (Cu or Ni foam), carbon-based materials and lithiophilic materials [115,116]. Xie *et al.* [117] demonstrated that the undesirable Li nucleation can be effectively inhibited by SnS_2, which can provide the nucleation seeds and control the growth direction of Li metal. Based on the "host" strategy, more space can be provided to withstand the volume changes for Li anode and suppress Li dendrite relative to the "hostless" strategies.

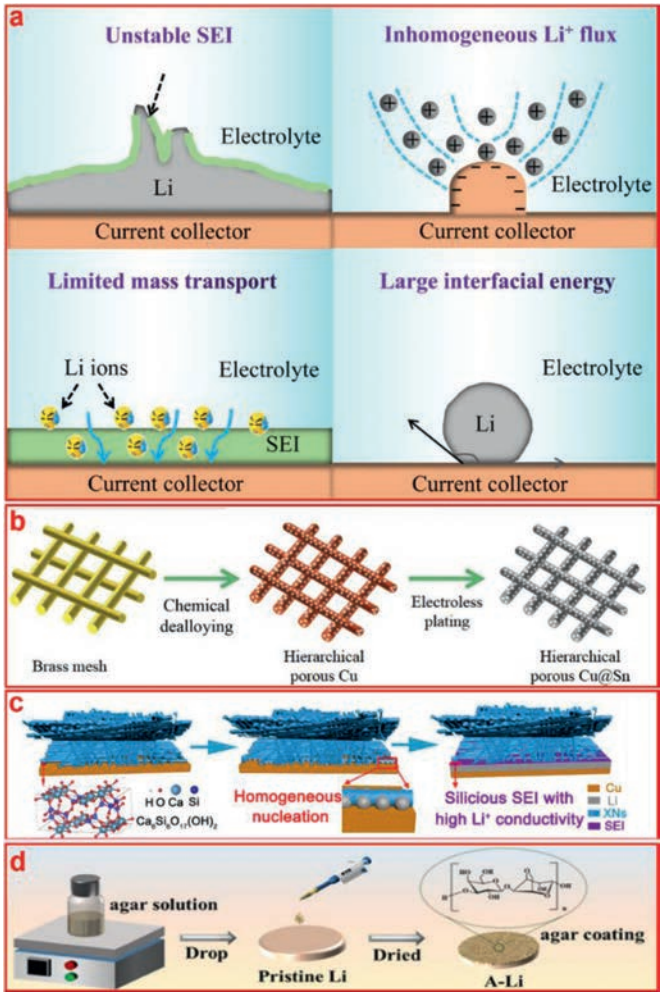

Fig. 8. (a) Scheme of the key interfacial challenges of Li anode in liquid electrolyte system. Reproduced with permission [110]. Copyright 2020, Elsevier. (b) The preparation process of HP-Cu@Sn current collector. Reproduced with permission [111]. Copyright 2020, Elsevier. (c) The scheme of Li nucleation and plating process on Cu or XNs protected Cu. Reproduced with permission [112]. Copyright 2021, Elsevier. (d) The process of the Li anode coated by agar. Reproduced with permission [114]. Copyright 2021, American Chemical Society.

5. Conclusions and future prospects

In this minireview, we have made a comprehensive summary about the recent progress and applications of metal-based 2D nanomaterials in Li-S system. Emphasis is placed on how to resolve inevitable issues associated with the utilization of the active material, reaction kinetics and the diffusion of polysulfides. Given that metal-based 2D nanomaterials have light weight, high conductivity and large surface area, it is very appealing to employ them as the host materials for S species, modified separator/interlayers and Li anode protection aiming at solving the low conductivity of S species, shuttle effect and the growth of Li dendrites in Li-S system. All of these strategies can greatly enhance the electrochemical properties of Li-S batteries [118]. However, compared with the traditional Li-ion batteries, Li-S batteries suffer from the low active S loading (<5 mg/cm^2), high E/S (electrolyte/sulfur) ratio (>1 μL/mg) and low energy density (<500 Wh/kg), which are mainly attributed to the poor conductivity of S cathode. Theoretically, these problems can be resolved by introducing electrocatalysts at the inner of Li-S batteries, including S host materials and interlayer/modified separator, which can entrap the dissolution and/or diffusion and accelerate the reaction kinetics of LiPSs [119]. In order to achieve the practical application of Li-S batteries, the S utilization and areal capacity of S should be improved to 80% and 6 mAh/cm^2, respectively. Especially, the long-term cycling stability should be up to 1000 cycles [120]. Unfortunately, there is no work satisfying all the parameters. In order to reach the last stage of practical Li-S batteries, the following aspects are necessary to be considered.

Firstly, at the materials level, metal-based 2D nanomaterials should be engineered further when used as host materials, interlayer/separator modification layer, and Li anode protection. Their microscopic structures and components (metal or non-metal sites) play significant roles in suppressing the shuttling effect and accelerating the conversion of LiPSs. On one hand, metal-based 2D nanomaterials with porous structures or ultrathin layer construction can provide large contact interface and rich reaction sites for hindering the migration and enhancing the catalytic activity for rapid conversion of LiPSs. This should be one of the main topics in the future, so as to achieve long-term cycling stability for the Li-S batteries. On the other hand, metal or non-metal reaction sites are very important in accelerating the reaction kinetics of Li-S batteries. Namely, the incorporation of metal and non-metal sites into single material can result in very strong synergistic effects for the adsorption and conversion of LiPSs by forming chemical bonds with S species. At present, N or O elements in metal-based 2D nanomaterials are found to have a great effect on preventing the leakage of LiPSs from the host materials due to the polar-polar interactions (between the Li^+ and polar units) [121]. However, these new reaction sites and the corresponding adsorption mechanisms are still an open question, which need to be uncovered by the combined theoretical calculations and *in-situ* techniques. Finally, in order to maximize atom utilization, the single-atom metal-based 2D nanomaterials should be paid much attention, where their reaction stoichiometry, reaction temperature and time, structure and morphology are the main factors to be optimized [122,123].

Secondly, at the cell level, the cooperative effects of different components, including S cathode, interlayer/modified separator and anode protection, should be taken into consideration comprehensively. To the best of our knowledge, all the components in the pouch cell, such as binder polymer, host materials, thickness of interlayer/modified separator, S active material, Li anode, should cooperate together to avoid the corrosion of Li anode, the formation of "dead Li" and fast capacity fading, so as to achieve high energy density for the Li-S batteries [123].

Binder polymer plays an important role in the electrical contact at the interfaces between S composite material and conductive additives, and fix the electrode materials onto the current collectors. At present, polyvinylidene fluoride (PVDF) is a conventional binder, but it has some inevitable disadvantages, such as weak interaction or adsorption with LiPSs, the presence of toxic solvents, *etc.* For the sake of achieving high areal capacity (6 mAh/cm^2, theoretical sulfur loading: 3.58 mg/cm^2), it is essential to design binder-free or self-standing S cathode in Li-S cell through layer-by-layer strategy, directing to greatly increasing the S content (>70%) in cathode [124].

To the best of our knowledge, a large amount of Li metal has been used for the anode thus far, which far exceeds the actually required dosage depending on the S cathode. Considering the high price and scarce reserves of Li on earth, an ideal anode should have low dosage of Li metal in the range of 0.43-0.86 mg Li per mg S to balance the charge of Li anode and S cathode [120]. To attain this goal, rational design and synthesis of metal-based 2D nanomaterials as the host materials for anchoring Li metal deserves deeply investigation.

To go a further step toward practical use, it is essential to use lean electrolytes for testing the pouch Li-S cell. Unfortunately, a high rate of electrolyte/sulfur is indispensable for current

research, meaning that there is a big gap between fundamental studies and real application. For example, carbon-based nanomaterials with large pore volume can improve the S loading, but excess electrolyte would be required to complete the electrode infiltration, resulting in low volume energy density [125]. Especially, at the lean electrolyte conditions (<5 μL/mg), the viscosity of electrolyte with dissolved LiPSs would rise gradually, resulting in slow transfer of Li^+ ion/electron and poor electrochemical properties [126]. In this regard, metal-based 2D nanomaterials show their advantages at the lean electrolyte conditions, including large space for high S loading and holding sufficient electrolyte, restraining spatially inhomogeneous electrochemical reactions. These advantages can be ascribed to the conductive network, reduced Li^+ diffusion distance and more active sites of the materials [127,128]. Thus, it is highly desirable to understand the reaction kinetics of S species under low electrolyte/sulfur conditions by means of *in-situ* spectroscopic techniques, so as to build some new strategies for preparing high-performance Li-S cell applied to lean electrolytes.

In general, metal-based 2D nanomaterials can be used in optimizing the S cathode, conducting additives and active materials (modifying the separator or Li anode) to solve the above challenges, and enhance the cycling performance in Li-S system. Specifically, in order to decrease the cost and safeguard human's environment, single-atom catalysts (SACs) of Fe-based, W-based or other non-noble-metal 2D nanomaterials with few-layers, flower-like or porous structures could be the best choice to trap the LiPSs by the electrocatalytic centers. In particular, the N_x sites present polar species for adsorbing LiPSs, which can be introduced at the surface of metal-based 2D nanomaterials. Consequently, combining metal-based 2D nanomaterials with metal-N_x sites is potentially an effective strategy to resolve the issues in Li-S system.

Declaration of competing interest

The authors declare no conflict of interest.

Acknowledgments

This work was supported by National Natural Science Foundation of China (No. 52172197), the Joint Funds of the National Natural Science Foundation of China (No. U1865207), Science and Technology Innovation Platform (No. 2018RS3070), Hundred Youth Talents Programs of Hunan Province, PhD Start-up Foundation of Hengyang Normal University (No. 19QD10), and Scientific Research Fund of Hunan Provincial Education Department (No. 20A062). We also thank the support from Hunan joint international laboratory of advanced materials and technology for clean energy (No. 2020CB1007) and the Science and Technology Innovation Program of Hunan Province (No. 2016TP1020).

References

[1] J. Deng, C. Bae, A. Denlinger, T. Miller, Joule 4 (2020) 509-515.
[2] P. Wang, B. Xi, M. Huang, et al., Adv. Energy Mater. 11 (2021) 2002893.
[3] Y.T. Liu, S. Liu, G.R. Li, X.P. Gao, Adv. Mater. 33 (2021) 2003955.
[4] C. Wang, L. Sun, L. Kai, et al., ACS Appl. Mater. Interfaces 12 (2020) 43560–43567.
[5] K.H. Su, P.W. Chi, T. Paul, et al., Mater. Today Phys. 18 (2021) 100373.
[6] J. Conder, R. Bouchet, S. Trabesinger, et al., Nat. Energy 2 (2017) 17069.
[7] S.S. Zhang, J. Power Sources 231 (2013) 153–162.
[8] R. Fang, S. Zhao, Z. Sun, et al., Adv. Mater. 29 (2017) 1606823.
[9] Q. Shao, Z.S. Wu, J. Chen, Energy Storage Mater. 22 (2019) 284–310.
[10] Z.W. Seh, W. Li, J.J. Cha, et al., Nat. Commun. 4 (2013) 1331.
[11] S. Tao, W.F. Huang, S.Q. Chu, et al., Mater. Today Phys. 18 (2021) 100403.
[12] J.X. Lin, Y.X. Mo, P.F. Zhang, et al., Mater. Today Energy 13 (2019) 267–276.
[13] Y. Wu, D. Lei, C. Wang, Mater. Today Phys. 18 (2021) 100395.
[14] S.Y. Liu, C.Y. Fan, Y.H. Shi, et al., ACS Appl. Mater. Interfaces 10 (2018) 509–516.
[15] M. Hagen, D. Hanselmann, K. Ahlbrecht, et al., Adv. Energy Mater. 5 (2015) 1401986.
[16] H. Hong, N. Mohamad, K. Chae, et al., J. Mater. Chem. A 9 (2021) 10012–10038.
[17] J. Nai, X. Zhao, H. Yuan, X. Tao, L. Guo, Nano Res. 14 (2021) 2053–2066.
[18] T. Li, C. He, W. Zhang, J. Energy Chem. 52 (2021) 121–129.
[19] X. Yang, G. Xia, J. Ye, W. Du, C. Hu, Appl. Surf. Sci. 22 (2021) 148632.
[20] F. Bonaccorso, L. Colombo, G. Yu, et al., Science 347 (2015) 1246501.
[21] J.S. Zeng, L. Zhang, Q. Zhou, et al., Small 18 (2022) 2104624.
[22] F.M. Cai, L.L. Liao, Y. Zhao, et al., J. Mater. Chem. A 9 (2021) 10199–10207.
[23] L.L. Liao, L. Yang, G. Zhao, et al., Chin. J. Chem. 39 (2021) 288–294.
[24] D.Y. Li, L.L. Liao, H.Q. Zhou, et al., Mater. Today Phys. 16 (2021) 100314.
[25] W. Xue, Z. Shi, L. Suo, et al., Nat. Energy 4 (2019) 374–382.
[26] L.L. Liao, J.Y. Sun, D.Y. Li, et al., Small 16 (2020) 1906629.
[27] C. Zhao, G.L. Xu, Z. Yu, et al., Nat. Nanotechnol. 16 (2021) 166–173.
[28] J.Y. Sun, F. Tian, F. Yu, et al., ACS Catal. 10 (2020) 1511.
[29] L. Shi, Z. Li, L.C. Ju, et al., J. Mater. Chem. A 8 (2020) 1059–1065.
[30] Q. Zhou, L.L. Liao, Q.H. Bian, et al., Small 18 (2022) 2105642.
[31] D.R. Deng, C. Bai, F. Xue, et al., ACS Appl. Mater. Interfaces 11 (2019) 11474–11480.
[32] J. Miao, C. Wang, Nano Res. 14 (2021) 1878–1888.
[33] L. Liao, C. Cheng, H. Zhou, et al., Mater. Today Phys. 22 (2022) 100589.
[34] X. Song, T. Zhang, H. Yang, H. Ji, H. Gao, Nano Res. 14 (2021) 3810–3819.
[35] Q. Li, Y. Liu, L. Yang, Y. Wang, B.J. Zhong, Colloid Interf. Sci. 585 (2021) 43–50.
[36] B. Bwa, A. Jh, A. Lz, Mater. Today Commun. 27 (2021) 102312.
[37] D. Xie, S. Mei, Y. Xu, et al., ChemSusChem 14 (2021) 1404–1413.
[38] T. Shi, C. Zhao, C. Yin, H. Yin, K. Yu, Nanotechnology 31 (2020) 495406.
[39] X. Zhou, J. Tian, Q. Wu, J. Hu, C. Li, Energy Storage Mater. 24 (2020) 644–654.
[40] C.P. Yang, Y.X. Yin, H. Ye, et al., ACS Appl. Mater. Interfaces 6 (2014) 8789–8795.
[41] X. Yang, Z. Meng, T. Ca, W.Q. Han, ACS Appl. Mater. Interfaces 7 (2015) 25202–25210.
[42] C. Jin, W. Zhang, Z. Zhuang, et al., J. Mater. Chem. A 5 (2017) 632–640.
[43] S. Zhang, D. Xu, C. Su, et al., Chem. Commun. 56 (2020) 810–813.
[44] S. Li, Q. Xiang, M.K. Aslam, et al., J. Electroanal. Chem. 850 (2019) 113408.
[45] J.H. Ahn, G.K. Veerasubramani, S.M. Lee, T.S. You, D.W. Kim, J. Electrochem. Soc. 166 (2019) A5201–A5209.
[46] Y. Zhang, G. Li, J. Wang, et al., Adv. Funct. Mater. 30 (2020) 2001165.
[47] J. Li, Y. Xu, Y. Zhang, C. He, T. Li, J. Mater. Chem. A 8 (2020) 19544–19554.
[48] H. Li, S. Ma, H. Cai, et al., Energy Storage Mater. 18 (2019) 338–348.
[49] Y. Qiu, L. Fan, M. Wang, et al., ACS Nano 14 (2020) 16105–16113.
[50] C. Song, Q. Jin, W. Zhang, et al., J. Colloid Interf. Sci. 595 (2021) 51–58.
[51] P. Zeng, C. Liu, X. Zhao, et al., ACS Nano 14 (2020) 11558–11569.
[52] Y. Zhu, G. Li, D. Luo, et al., Nano Energy 79 (2021) 105393.
[53] J. He, A. Bhargav, A. Manthiram, ACS Nano 15 (2021) 8583–8591.
[54] G.M. Zhou, S.Y. Zhao, T.S. Wang, et al., Nano Lett. 20 (2020) 1252–1261.
[55] C.G. Wang, H.W. Song, C.C. Yu, et al., J. Mater. Chem. A 8 (2020) 3421–3430.
[56] Z.Z. Liu, L. Zhou, Q. Ge, et al., ACS Appl. Mater. Interfaces 10 (2018) 19311–19317.
[57] H. Wang, T. Zhou, D. Li, et al., ACS Appl. Mater. Interfaces 9 (2016) 4320–4325.
[58] H. Zhang, M. Zou, W. Zhao, et al., ACS Nano 13 (2019) 3982–3991.
[59] J. Wei, H. Su, C. Qin, et al., J. Electroanal. Chem. 837 (2019) 184–190.
[60] J. Pu, Z. Shen, J. Zheng, et al., Nano Energy 37 (2017) 7–14.
[61] Z.Y. Wang, L. Wang, S. Liu, G.R. Li, X.P. Gao, Adv. Funct. Mater. 29 (2019) 1901051.
[62] X. Song, D. Tian, Y. Qiu, et al., Energy Storage Mater. 41 (2021) 248–254.
[63] W. Ren, M. Wei, U.M. Muhammad, et al., ChemSusChem 11 (2018) 2695–2702.
[64] X. Zhang, Y. Tian, W. Lu, et al., ChemElectroChem 8 (2021) 3629–3636.
[65] Y.X. Mo, J.X. Lin, Y.J. Wu, et al., ACS Appl. Mater. Interface 11 (2019) 4065–4073.
[66] Z. Sun, S. Vijay, H.H. Heenen, et al., Adv. Energy Mater. 10 (2020) 1904010.
[67] X. Yang, G. Xia, J. Ye, et al., Appl. Surf. Sci. 22 (2021) 148632.
[68] B. Guan, Y. Zhang, L. Fan, et al., ACS Nano 13 (2019) 6742–6750.
[69] W. Sun, Y. Li, S. Liu, et al., Chem. Eng. J. 416 (2021) 129166.
[70] Z. Zhuang, Q. Kang, D. Wang, Y. Li, Nano Res. 13 (2020) 11.
[71] Z.Z. Du, X.J. Chen, W. Hu, et al., J. Am. Soc. Chem. 141 (2019) 3977–3985.
[72] M. Wang, L. Fan, X. Sun, et al., ACS Energy Lett. 5 (2020) 3041–3050.
[73] Y. Wang, J. Shen, L.C. Xu, et al., Phys. Chem. Chem. Phys. 21 (2019) 18559.
[74] S. Liu, C. Zhang, W. Yue, X. Chen, X. Yang, ACS Appl. Energy Mater. 2 (2019) 5009–5018.
[75] R. Meng, Q. Deng, C. Peng, et al., Nano Today 35 (2020) 100991.
[76] J. He, A. Bhargav, A. Manthiram, Adv. Mater. 32 (2020) 2004741.
[77] W. Yang, W. Yang, L. Dong, et al., J. Mater. Chem. A 7 (2019) 13103–13112.
[78] J. Liu, S. Xiao, L. Chang, et al., J. Energy Chem. 56 (2021) 343–352.
[79] H.Y. Zhou, Z.Y. Sui, K. Amin, et al., ACS Appl. Mater. Interfaces 12 (2020) 13904–13913.
[80] H. Shi, J. Qin, P. Lu, et al., Adv. Funct. Mater. 31 (2021) 2102314.
[81] J. Zhang, C. You, H. Lin, J. Wang, Energy Environ. Mater. 5 (2022) 731–750.
[82] J.J. Yuan, Z. Huang, Y.Z. Song, M.Y. Li, H.Y. Li, Chem. Eng. J. 426 (2021) 128705.
[83] D. Luo, Z. Zhang, G. Li, et al., ACS Nano 14 (2020) 4849–4860.
[84] Z. Qiao, Y. Zhang, Z. Meng, et al., Adv. Funct. Mater. 31 (2021) 2100970.
[85] C. Ma, Y. Zhang, Y. Feng, et al., Adv. Mater. 33 (2021) 2100171.
[86] Y.J. Zhang, J. Qu, Q.Y. Ji, et al., Carbon 155 (2019) 353–360.
[87] H. Pan, Z. Tan, H. Zhou, et al., J. Energy Chem. 39 (2019) 101–108.
[88] H. Yang, Y. Yang, X. Zhang, et al., ACS Appl. Mater. Interfaces 11 (2019) 31860–31868.
[89] Z. Zhao, Z. Yi, H. Li, R. Pathak, Z. Yang, et al., Nano Energy 81 (2021) 105621.
[90] X. Li, X. Yang, J. Ye, G. Xia, Z. Fu, et al., Chem. Eng. J. 405 (2021) 126947.
[91] Y. Wang, L. Yang, Y. Chen, et al., ACS Appl. Mater. Interfaces 12 (2020) 57859–57869.

[92] B. Guan, X. Sun, Y. Zhang, et al., Chin. Chem. Lett. 32 (2021) 2249–2253.
[93] Y. Hu, A. Hu, J. Wang, et al., J. Mater. Chem. A 9 (2021) 9771–9779.
[94] J.X. Lin, X.M. Qu, X.H. Wu, et al., ACS Sustainable Chem. Eng. 9 (2021) 1804–1813.
[95] J. Wang, W. Cai, X. Mu, et al., Nano Res. 14 (2021) 4865–4877.
[96] J. Xie, B. Li, H. Peng, et al., Adv. Mater. 31 (2019) 1903813.
[97] Y. Zhang, X. Liu, L. Wu, et al., J. Mater. Chem. A 8 (2020) 2741–2751.
[98] P. Li, H. Lv, Z. Li, et al., Adv. Mater. 33 (2021) 2007803.
[99] J. Cui, Z. Li, J. Li, et al., J. Mater. Chem. A 8 (2020) 1896–1903.
[100] Z. Chang, Y. Qiao, J. Wang, H. Deng, H.J. Zhou, J. Mater. Chem. A 9 (2021) 4870–4879.
[101] P. Wang, B. Xi, Z. Zhang, et al., Angew. Chem. Int. Ed. 60 (2021) 15563–15571.
[102] Y. Tian, G. Li, Y. Zhang, et al., Adv. Mater. 32 (2019) 1904876.
[103] C. Chao, Q. Jiang, H. Xu, et al., Nano Energy 76 (2020) 105033.
[104] N. Li, Y. Xie, S. Peng, X. Xiong, K. Han, J. Energy Chem. 42 (2020) 128–137.
[105] K. Xu, X. Liang, L.L. Wang, et al., Rare Met. 40 (2021) 2810–2818.
[106] X. Liu, G. Feng, Y. Li, et al., Ind. Eng. Chem. Res. 59 (2020) 7538–7545.
[107] P. Cheng, P. Guo, K. Sun, et al., J. Membrane Sci. 619 (2021) 118780.
[108] G. Yan, C. Xu, Z. Meng, et al., Nanoscale 12 (2020) 24368–24375.
[109] W. Tian, B. Xi, Y. Gu, et al., Nano Res. 13 (2020) 2673–2682.
[110] Z. Luo, X. Qiu, C. Liu, et al., Nano Energy 79 (2021) 105507.
[111] Z. Luo, C. Liu, Y. Tian, et al., Energy Storage Mater. 27 (2020) 124–132.
[112] Y. Liu, Y. Wu, J. Zheng, et al., Nano Energy 82 (2021) 105723.
[113] L. Xue, W. Chen, Y. Hu, et al., Nano Energy 79 (2021) 105481.
[114] C. Cui, R. Zhang, C. Fu, et al., ACS Appl. Mater. Interfaces 13 (2021) 28252–28260.
[115] K. Yan, Z. Lu, H.W. Lee, et al., Nat. Energy 1 (2016) 16010.
[116] S.S. Chi, Q. Wang, B. Han, et al., Nano Lett. 20 (2020) 2724–2732.
[117] D. Xie, H.H. Li, W.Y. Diao, et al., Energy Storage Mater. 27 (2020) 124–132.
[118] J. Wang, S. Yi, J. Liu, et al., ACS Nano 14 (2020) 9819–9831.
[119] M. Gao, W.Y. Zhou, Y.X. Mo, et al., Adv. Powder Mater. 1 (2022) 100006.
[120] R. Deng, M. Wang, H. Yu, et al., Energy Environ. Mater. 5 (2022) 777–799.
[121] M. Jana, R. Xu, X.B. Cheng, et al., Energy Environ. Sci. 13 (2020) 1049–1075.
[122] J. Mei, T. Liao, Z. Sun, Energy Environ. Mater. 4 (2021) 1–18.
[123] Y. Cao, X. Meng, A. Li, Energy Environ. Mater. 4 (2021) 363–391.
[124] M.A. Pope, I.A. Aksay, Adv. Energy Mater. 5 (2015) 1500124.
[125] S.F. Ng, M.Y.L. Lau, W.J. Ong, Adv. Mater. 33 (2021) 2008654.
[126] M. Zhao, B. Li, X. Zhang, J. Huang, Q. Zhang, ACS Cent. Sci. 6 (2020) 1095–1104.
[127] L. Cong, H. Xie, J. Li, Adv. Energy Mater. 7 (2017) 1601906.
[128] S.W. Song, L. Yu, X. Xiao, et al., Mater. Today Phys. 13 (2020) 100216.